

## Characterization of interfacial roughness in Co/Cu multilayers by x-ray scattering

T. Gu and A. I. Goldman

Ames Laboratory-USDOE and Department of Physics and Astronomy, Iowa State University, Ames, Iowa 50011

M. Mao\*

Department of Physics & Astronomy, McMaster University, Hamilton, Ontario, Canada L8S 4M1

(Received 6 March 1997)

The interfacial roughness of a magnetron-sputtered Si(001)/[Co 12 Å/Cu 9.7 Å]<sub>30</sub>/(Cu 30 Å) multilayer was investigated by x-ray scattering, and partial conformal roughness was observed. Specular, longitudinal, and transverse diffuse intensities were acquired by a high-resolution triple-crystal x-ray diffractometer and evaluated simultaneously based on the distorted-wave Born approximation. An approach to the analysis of the diffuse signal is proposed. [S0163-1829(97)07235-4]

Recent years have witnessed an increasing interest in the morphology of multilayer interfaces since the interfaces play a crucial role in determining the physical properties of multilayers. For instance, in magnetic multilayers exhibiting giant magnetoresistance (GMR), it is understood that the interfacial structure will affect the completeness of anti-ferromagnetic exchange coupling between the ferromagnetic layers and, therefore, influences the GMR effect.<sup>1</sup>

X-ray scattering has been widely used as a nondestructive method to probe buried interfaces. Specular and nonspecular reflectivities from x-ray-scattering measurements contain statistical information about the interfacial structure which can be accessed by employing a model based on the distorted-wave Born approximation (DWBA) to evaluate the reflectivity data.<sup>2-4</sup> Furthermore, the growth behavior during the deposition can be deduced.<sup>5</sup>

In this article, we report our observation and characterization of the conformal growth of Co/Cu multilayers fabricated by magnetron sputtering. This system presents a relatively large GMR at room temperature, and is one of the most suitable candidates for technical applications.<sup>6</sup> The mutual immiscibility of the two materials is expected to help form sharp interfaces and may enhance interfacial phenomena.

Previous work, by x-ray diffraction, on molecular-beam-epitaxy- (MBE-) grown Co/Cu multilayers, has shown that Co and Cu layers grow predominantly along the (111) direction.<sup>7,8</sup> Reflectivity measurements of epitaxially grown Cu/Co multilayers have been reported, but did not address the issue of conformal growth in this system.<sup>7</sup> Recent studies on Co/Cu interfaces, however, indicate that conformal growth in this system may not be likely since the roughness of Co/Cu interfaces is different from that of Cu/Co interfaces.<sup>9,10</sup> Other experiments have demonstrated the existence of conformal roughness in a related system of NiFeCo/Cu multilayers.<sup>11</sup> Here, we describe measurements of the specular and nonspecular reflectivity of a Cu/Co multilayer, using a high-resolution triple-crystal diffractometer. The novelty of our method lies in the simultaneous analysis of two-dimensional data: the specular reflectivity, and several lateral and longitudinal diffuse components, with each data set collected in such a way that it contains the information featuring different structural signatures. In this

manner, the analysis will lead to self-consistent and more accurate determination of structural parameters. The algorithm developed for simultaneous fitting using the DWBA will be presented elsewhere. Here we outline our general approach and its utility for studying conformal growth in the Co/Cu multilayer system.

According to the DWBA, the specular part of the scattered intensity reflects the average interface structure of the system. Interfacial roughness serves as a perturbation to the mean system, and the cross section for diffuse scattering is given by<sup>3,12</sup>

$$\left(\frac{d\sigma}{d\Omega}\right)_{\text{dif}} = \frac{Sk^4}{16\pi^2} \sum_{j,k=1}^N (n_j^2 - n_{j+1}^2)(n_k^2 - n_{k+1}^2)^* \sum_{m,n=0}^3 E_j^m E_k^{n*} \times \exp\{-0.5[(q_{z,j}^m \sigma_j)^2 + (q_{z,k}^n \sigma_k)^2]^*\} \frac{G_{jk}^{mn}}{q_{z,j}^m q_{z,k}^{n*}},$$

where  $k$  is the wave vector of incident x rays;  $n_j$  is the refractive index of the material beneath the  $j$ th interface;  $E_j^m$  represents the transmitted ( $T$ ) and reflected ( $R$ ) electric fields (distorted waves) at the  $j$ th interface:  $E_j^0 = T_j^s T_j^d$ ,  $E_j^1 = T_j^s R_j^d$ ,  $E_j^2 = R_j^s T_j^d$ ,  $E_j^3 = R_j^s R_j^d$  with  $s$  and  $d$  denoting source and detector directions. The  $q_{z,j}$  are the normal components of  $\mathbf{q}$  beneath the  $j$ th interface with  $\mathbf{q}_j^0 = \mathbf{k}_j^s + \mathbf{k}_j^d$ ,  $\mathbf{q}_j^1 = \mathbf{k}_j^s - \mathbf{k}_j^d$ ,  $\mathbf{q}_j^2 = -\mathbf{q}_j^1$ ,  $\mathbf{q}_j^3 = -\mathbf{q}_j^0$ ;  $N$  is the number of interfaces,  $\sigma$  the root-mean-square (rms) roughness, and  $S$  the illuminated area of the surface. The factor  $G$  is

$$G_{jk}^{mn} = \int \{ \exp[q_{z,j}^m q_{z,k}^{n*} C_{jk}(x,y)] - 1 \} \times \exp[-i(q_x x + q_y y)] dx dy,$$

where  $C_{jk} = \langle l_j(0,0) l_k(x,y) \rangle$  represents the average value of the height-height correlations between the  $j$ th interface of height  $l_j$  and the  $k$ th interface of height  $l_k$ . By studying diffuse reflectivity, one can measure the parameters contained in the correlation functions.

It is shown, by the above formulas, that the diffuse intensity depends not only on the factor  $G_{jk}$  but also on the fields  $E_j E_k$ .  $R$  and  $T$  contained in the fields may both be appre-

cialable at a Bragg peak around which the diffuse signals are usually evaluated. For a given  $q_z$ , the fields  $E_j E_k$  are a function of  $q_{\parallel} = \sqrt{q_x^2 + q_y^2}$  and will generally influence the profile of the diffuse intensity. This effect manifests itself more pronouncedly on the diffuse intensities around higher-order Bragg peaks in the form of *Umweganregung* or multiple scattering.<sup>4,11,13</sup> It is, therefore, important to consider the influence of specular intensity upon the evaluation of the diffuse signal by fitting the specular and diffuse intensities simultaneously.

By assuming a self-affine isotropic surface, the *self height-height correlation function*  $C_{jj}$  can be expressed as

$$C_{jj} = \sigma_j^2 \exp[-(r/\xi_j)^{2h_j}],$$

where  $r$  is the magnitude of a position vector  $\mathbf{r}$  in the surface, and  $\sigma$ ,  $h$ , and  $\xi$  are the root-mean-square roughness, roughness exponent, and lateral correlation length of the surface, respectively. The concept of conformality arises when the *cross-correlation function*  $C_{jk}$ ,  $j \neq k$ , is considered for heterostructure growth. As introduced by Stearns,<sup>14</sup> conformal growth describes the case where the roughness spectrum of a newly grown interface replicates that of one deposited earlier. Mathematically, the cross-correlation function can be presented as

$$C_{jk} = a_{jk} C_{jj}, \quad k \neq j,$$

where  $C_{jj}$  is the self-correlation function of the  $j$ th interface. The factor  $a_{jk}$  is generally a function of the distance between the  $j$ th and  $k$ th layers, and is related to the *vertical correlations*  $\xi_{\perp}$  of the system. In reality, the degree of conformality may vary, for instance, as a function of lateral scale, since replication usually functions as a low-frequency bandpass filter.<sup>15,16</sup>

Both DWBA and the Born approximation predict that, if the roughness has a certain degree of conformality, the diffuse intensity concentrates, in reciprocal space, around  $q_z = m2\pi/\Lambda$ , where  $m$  is an integer and  $\Lambda$  is the periodicity of the multilayer, and forms a ‘‘Bragg sheet.’’<sup>4,14,17</sup> Under this condition, the resonant fields at the interfaces coherently enhance the diffuse signal. The thickness of the sheet is determined by the number of correlated layers and, therefore, by the vertical correlation length. It may vary according to the spectral frequency in the interface plane such as  $q_x$ .<sup>15</sup> For instance, it is known that a desorption-governed surface diffusion during deposition will give a  $q_x^{-2}$ -dependent  $\xi_{\perp}$ , while a  $q_x^{-4}$ -dependent  $\xi_{\perp}$  implies a diffusion caused by local chemical potential difference.<sup>18,19</sup>

For our study, a multilayer of Si(001)/[Co 12 Å/Cu 9.5 Å]<sub>30</sub>/(Cu 30 Å) was prepared by dc magnetron sputtering. The base pressure was  $8 \times 10^{-7}$  Torr, and the sample was grown under an argon pressure of  $1.25 \times 10^{-3}$  Torr. The deposition rate for both Co and Cu was about 1.5 Å/s. The substrate was held at room temperature.

The measurements were carried on a standard triple-crystal diffractometer with Ge(111) crystals as monochromator and analyzer. An 18-kW rotating-anode x-ray generator with a Cu target served as the source. Since, at low angles, the resolution is mainly limited by the Cu  $K_{\alpha}$  doublet separation,<sup>20</sup> a slit of width 0.5 mm was placed 50 cm after the monochromator to block the  $K_{\alpha 2}$  line. Another slit of

width 0.3 mm was placed after the analyzer to further tighten the resolution and reduce its influence upon the diffuse scattering.

In the modeling, it is assumed that the detector window fully integrates the scattering out of plane, which is also defined as the  $q_y$  direction, while the scattering plane is described by  $q_x$  and  $q_z$ , with  $q_z$  perpendicular to the sample surface. We use the simplified Epstein solution<sup>12,21,22</sup> to describe the reflection coefficient of a single interface and the Parrat formalism to recursively obtain the total specular reflectivity.<sup>23</sup>

Because the total thickness of the sample is  $\sim 700$  Å and the resolving power of the diffractometer at  $2\theta \sim 0^\circ$  is about  $10^{-3}$  Å, the instrumental resolution has been taken into consideration in modeling the longitudinal scans. This correction proved to be necessary.

In the data analysis, we noticed that it is important to treat the top layer and the bottom layer differently from the rest of the structure. This is due to the fact that the reaction between the first deposited layer and the substrate may significantly change the interfacial structure. Similarly, oxidation and contamination of the capping layer will also alter its structure. To limit the number of fitting parameters, we assume, however, that every interface may be characterized by a single roughness exponent  $h$  and lateral correlation length  $\xi$ . We also assume the Co/Cu and Cu/Co interfaces have different rms roughness parameters, and each type of interface has only one rms roughness parameter regardless of its relative position in the stacking.

The cross-correlation functions can be written as

$$C_{jk} = \sigma_j \sigma_k \exp(-d_{jk}/\xi_{\perp}) \exp[-(r/\xi)^{2h}],$$

where  $d_{jk}$  is the distance between the  $j$ th and  $k$ th layer.<sup>24</sup> The *mean vertical correlation length*  $\xi_{\perp}$  may be written in a more general form for small  $q_x$ :

$$\frac{1}{\xi_{\perp}} \approx \frac{1}{\xi_{\perp 0}} + \nu_p q_x^{2p}, \quad p = 1, 2, \quad q_x \ll 1,$$

with  $\nu_p$  the mean relaxation parameter indicating the surface diffusion and  $\xi_{\perp 0}$  a  $q_x$ -independent parameter. Its existence is justified by considering the fact that at  $q_x = 0$  the vertical correlation length should be finite. A recent experiment also demonstrated the evidence of the  $q_x$ -independent term.<sup>25</sup>

Figure 1 shows the specular data, diffuse data, and their simultaneously fit curves. Since the data measured are symmetric about the specular ridge, only the data for  $q_x > 0$  are modeled for longitudinal diffuse intensities. The fitting parameters are given in Table I.

The quality of the fit shown in Fig. 1 indicates that the model works very well. The rapidly oscillating part of the specular reflectivity is caused by the interference between the top surface and the multilayer-substrate interface. The broad envelope is due to the oxidation in the capping layer. Just above the Bragg peak, the fit curve deviates slightly from the experimental data. It was noticed during the fit that this section is sensitive to the structure of the bottom layer of the multilayer and may mean that this layer is not modeled perfectly. A model allowing for accumulative roughness was tested, and the fit was not improved. This indicates that the roughness of the system is not accumulative.

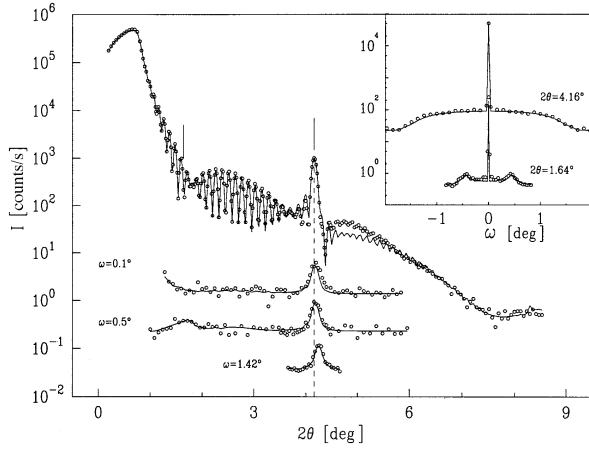


FIG. 1. The experimental data (open circles) and their simultaneous fits (solid lines). A vertical dashed line serves to indicate the bent Bragg sheet. The inset illustrates two transverse diffuse scans taken at different  $2\theta$  angles shown by two short lines above the specular curve.  $2\theta = \theta_1 + \theta_2$  and  $\omega = \theta_1 - 0.5(2\theta)$ , where  $\theta_1$  and  $\theta_2$  are the incident and exiting angles of the beam. In  $q_x$ - $q_z$  representation,  $q_x$  is along the  $\omega$  direction with  $q_x = k(\cos\theta_1 - \cos\theta_2)$ , and  $q_z$  is along the  $2\theta$  direction with  $q_z = 2k\sin[0.5(\theta_1 + \theta_2)]$ .

The Bragg sheet is clearly visible in the longitudinal diffuse scans. The sheet is bent: At larger  $q_x$  the sheet center shifts to higher  $q_z$ , as predicted by the dynamical scattering theory.<sup>4</sup> For different  $q_x$  the thickness of the Bragg sheet is slightly different, reflecting a varied number of correlated layers. In the fit, various  $p$  values were used. With all  $\nu_p = 0$ , the Bragg sheet can be fit fairly well except the systematic broadening of the sheet. An inclusion of the  $q_x$  term with  $p = 1$  gives the best fit with  $\nu_p = 7 \pm 1$  and  $\xi_{\perp 0} = 1200 \text{ \AA}$ . Since the current maximum  $q_x$  is about  $0.01 \text{ \AA}^{-1}$ , the magnitude and relative independence of  $\xi_{\perp}$  upon  $q_x$  indicate that a roughness with wavelength greater than  $2\pi/q_x \sim 600 \text{ \AA}$  is

TABLE I. Results obtained from fitting.  $\rho$  is the effective electron density in number of electrons per cubic angstrom. For comparison, bulk values are  $\rho_{\text{Co}} = 2.21$ ,  $\rho_{\text{Cu}} = 2.28$  at  $\lambda = 1.54059 \text{ \AA}$ .  $\sigma$  is the rms roughness and  $\beta$  is the linear absorption coefficient.  $d$  is the thickness in angstroms. Co (Cu) is the interface with Cu (Co) on the top of the Co (Cu) layer. Parameters not listed in the table are roughness exponent  $h = 0.7 \pm 0.2$ ,  $\xi = 17 \pm 3 \text{ \AA}$ . The roughness exponent is not very sensitive in the fitting. It mainly affects the relative diffuse intensities at high and low  $2\theta$  values.

	$\rho$ (electrons/ $\text{\AA}^3$ )	$\sigma$ ( $\text{\AA}$ )	$\beta \times 10^{-7}$	$d$ ( $\text{\AA}$ )
Top1	$1 \pm 0.1$	$6.4 \pm 0.3$	0 <sup>a</sup>	$27.3 \pm 0.5$
Top2(Cu)	2.4 <sup>a</sup>	$14 \pm 1$	6 <sup>a</sup>	$20 \pm 1$
Co	$2.2 \pm 0.1$	$6.2 \pm 0.4$	$43 \pm 1$	$12.3 \pm 0.3$
Cu	$2.3 \pm 0.1$	$6.4 \pm 0.6$	4.4	$9.1 \pm 0.3$
Bottom1	$2.8 \pm 0.3$	$15 \pm 3$	38	$12.4 \pm 0.3$
Bottom2	$0.97 \pm 0.05$	$3.6 \pm 0.3$	0.4 <sup>b</sup>	$16 \pm 0.6$
Si(sub)	0.68 <sup>c</sup>	$1 \pm 0.5$	1.2 <sup>c</sup>	n.a.

<sup>a</sup>Values hit limits during the fitting.

<sup>b</sup>Not sensitive in the fitting.

<sup>c</sup>Theoretical values are used.

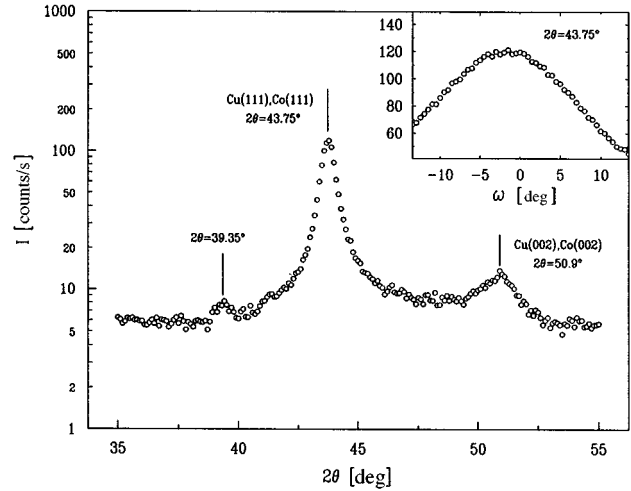


FIG. 2. The higher-angle data demonstrates a polycrystalline structure. The inset shows a broad  $\omega$  rocking curve. The small satellite peak at  $2\theta = 39.35^\circ$  is caused by superlattice modulation. It should separate from the Cu(111) peak by  $\Delta 2\theta = \lambda / (\Lambda \cos\theta) \approx 4.4^\circ$ , where  $\lambda = 1.54059 \text{ \AA}$  is the probing wavelength, and  $\Lambda = 21.47 \text{ \AA}$  is the periodicity of the multilayer. Destruction of interfacial stacking coherency makes it very weak.

mostly duplicated throughout the sample. In the current case,  $q_x^2$  term functions as a higher-order correction.

The inset of Fig. 1 illustrates transverse scans through the diffuse scattering. At the smaller- $2\theta$ -angle scan, rough interfaces cause Yoneda wings to appear, where the incident angle or exiting angle of x rays approaches the critical angle of the multilayer. The transverse scan across the Bragg peak at  $q_z = 2\pi/\Lambda$  has no visible Yoneda wings, since at higher  $2\theta$  Yoneda wings are usually weak due to a large  $\theta$  value in one of the two transmission coefficients  $T_j^s, T_j^d$ . This scan also shows that the diffuse intensity is very broad and flat, indicating a short lateral correlation length.

Since Co and Cu have a lattice mismatch of about 2% and a lattice constant about  $3.5 \text{ \AA}$ , one would expect a  $\xi$  about  $150 \text{ \AA}$  for epitaxially grown samples. The fit gives  $\xi$  of about  $17 \text{ \AA}$ . A small lateral characteristic size  $\xi$  of a system usually means a short diffusion length during the deposition, and will result in an imperfect stacking of the lattice in the system.

To further support this argument, we used high-angle x-ray diffraction to probe the structure at smaller length scales. In order to have higher flux, the Ge crystals were replaced with graphite. Figure 2 presents the high-angle data. In sharp contrast to epitaxially grown multilayers,<sup>7</sup> broader longitudinal peaks and an almost flat  $\omega$  rocking curve are observed. Together with the fact that both (111) and (002) peaks for Co and Cu are present and only one weak satellite peak shows up at  $2\theta = 39.35^\circ$  due to superlattice modulation, we can deduce that the orientation of polycrystalline Cu and Co is fairly random and therefore effectively reduces the coherency of stacking and the lateral correlations. This together with small  $\xi$  value provides evidence for a strong nonequilibrium growth mechanism during the sample deposition.<sup>19</sup>

In conclusion, a conformal growth in a magnetron-sputtered Co/Cu multilayer was observed and characterized.

Both specular and diffuse x-ray-scattering data were fit simultaneously according to the DWBA. This measurement helps to impose more constraints on the evaluation of the multilayer structure. In addition to layer thickness and rms roughness, we also acquired a lateral correlation length of about 17 Å and a roughness exponent of 0.7. The roughness is largely duplicated through the whole sample. The existence of a  $q_x^2$ -dependent term in  $\xi_{\perp}^{-1}$ , though a higher-order correction, indicates a damping effect on the propagation of high-frequency roughness during the growth. The higher-angle scattering data revealed a textured polycrystalline microstructure of the multilayer and a lack of interface coher-

ency characterized by the absence of strong superlattice modulation satellite peaks. This is consistent with the short lateral correlation length observed in the low-angle scattering. By incorporating the information from both high- and low-angle scattering, we have a comprehensive picture of the interfacial structure.

We would like to thank Professor M. Sutton at the Department of Physics, McGill University, Canada, for many useful discussions and help. This work was supported by Ames Laboratory which is operated for the U.S. Department of Energy by Iowa State University under Contract No. W-7405-Eng-82.

\*Present address: Lawrence Livermore National Laboratory, P.O. Box 808, Livermore, CA 94551.

<sup>1</sup>S.S.P. Parkin, in *Ultrathin Magnetic Structures II*, edited by B. Heinrich and J.A.C. Bland (Spring-Verlag, Berlin, 1994).

<sup>2</sup>S.K. Sinha, E.B. Sirota, S. Garoff, and H.B. Stanley, *Phys. Rev. B* **38**, 2297 (1988).

<sup>3</sup>J. Daillant and O. B elorgey, *J. Chem. Phys.* **98**, 5824 (1992).

<sup>4</sup>V. Hol y and T. Baumbach, *Phys. Rev. B* **49**, 10 668 (1994).

<sup>5</sup>See, for example, C. Thompson, G. Palasantzas, Y.P. Feng, S.K. Sinha, and J. Krim, *Phys. Rev. B* **49**, 10 668 (1994).

<sup>6</sup>S.S.P. Parkin, Z.G. Li, and D.J. Smith, *Appl. Phys. Lett.* **58**, 2710 (1991).

<sup>7</sup>P. B odeker, A. Abromeit, K. Br ohl, P. Sonntag, N. Metoki, and H. Zabel, *Phys. Rev. B* **47**, 2353 (1993).

<sup>8</sup>F.J. Lamelas, C.H. Lee, H. He, W. Vavra, and R. Clarke, *Phys. Rev. B* **40**, 5839 (1989).

<sup>9</sup>Th. Eckl, G. Reiss, H. Br uckl, and H. Hoffmann, *J. Appl. Phys.* **75**, 362 (1994).

<sup>10</sup>T.J. Minvielle and R.J. Wilson, *Appl. Phys. Lett.* **68**, 2750 (1994).

<sup>11</sup>Z.T. Diao, K. Meguro, S. Tsunashima, and M. Jimbo, *Phys. Rev. B* **53**, 8227 (1996).

<sup>12</sup>J. Stettner, L. Schwalowsky, O.H. Seeck, M. Tolan, W. Press, C. Schwarz, and H.V. K anel, *Phys. Rev. B* **53**, 1398 (1996).

<sup>13</sup>D.E. Savage, J. Kleiner, N. Schimke, Y.-H. Phang, T. Jankowski, J. Jacobs, R. Kariotis, and M.G. Lagally, *J. Appl. Phys.* **69**, 1411 (1994).

<sup>14</sup>D.G. Stearns, *J. Appl. Phys.* **71**, 4286 (1992).

<sup>15</sup>E. Spiller, D. Sterns, and M. Krumrey, *J. Appl. Phys.* **74**, 107 (1993).

<sup>16</sup>T. Salditt, H.M. Metzger, and J. Peosl, *Phys. Rev. Lett.* **73**, 2228 (1994).

<sup>17</sup>V.M. Kaganer, S.A. Stepanov, and R. K ohler, *Physica B* **221**, 34 (1996).

<sup>18</sup>M. Kardar, *Physica B* **221**, 60 (1996).

<sup>19</sup>A.L. Barab asi and H.E. Stanley, *Fractal Concepts in Surface Growth* (Cambridge University Press, Cambridge, England, 1995).

<sup>20</sup>T. Gu, Ph.D. thesis, McGill University, 1994.

<sup>21</sup>P.S. Epstein, *Proc. Natl. Acad. Sci. USA* **16**, 627 (1930).

<sup>22</sup>A. Caticha, *Phys. Rev. B* **52**, 9214 (1995).

<sup>23</sup>L.G. Parrat, *Phys. Rev.* **95**, 359 (1954).

<sup>24</sup>Z.H. Ming, A. Korl, Y.L. Soo, Y.H. Kao, J.S. Park, and K.L. Wang, *Phys. Rev. B* **47**, 16 373 (1993).

<sup>25</sup>T. Salditt, D. Lott, T.H. Metzger, J. Peisl, G. Vignaud, J.F. Legrand, G. Gr ubel, P. H ogh oi, and O. Sch arpf, *Physica B* **221**, 13 (1996).